Three-Dimensional Lattice Connectivities from Two-Dimensional High-Resolution Solid-State NMR. ^{29}Si MAS NMR Investigation of the Silicate Lattice of Zeolite ZSM-39 (Dodecasil 3C)

C. A. Fyfe,* H. Gies,*,† and Y. Feng

Contribution from the Department of Chemistry, University of British Columbia, Vancouver, British Columbia, Canada V6T 1Y6. *Received December 5, 1988*

Abstract: The potential of 2D ^{29}Si high-resolution solid-state NMR spectroscopy to establish three-dimensional Si/O/Si lattice connectivities in zeolites has been investigated using a ^{29}Si-enriched sample of zeolite ZSM-39. Spin-diffusion measurements reveal the correct connectivities for the (known) structure, but further work on other systems will be needed to establish the reliability of these measurements due to possible contributions from non-distance-dependent factors. ^{29}Si COSY experiments also yield the correct connectivities and are unambiguous in this regard as they depend only on scalar (through-bond) couplings and thus greatly extend the potential of high-resolution solid-state NMR in the investigation of lattice structures.

Zeolites are porous aluminosilicates (tectosilicates) whose unique 3D tetrahedral framework structures incorporate cavities and interconnecting channel systems, which gives them a size and shape selectivity for sorbed organic molecules.[1] This makes them of considerable importance in industry as molecular sieves and catalysts.[2] These materials are highly crystalline and their structures are often highly symmetrical, but there are difficulties in determining their crystal structures by diffraction techniques. First, they are usually microcrystalline with particle dimensions of a only few micrometers, which precludes the use of single-crystal diffraction techniques, and recourse must be made to much more limited powder diffraction data analysis.[3] Second, Si and Al atoms have very similar scattering factors and are often disordered within the framework of the lattice so that, even when the topology of the overall crystal structure is found, it is generally not possible to locate the Si and Al atoms within the framework.

High-resolution NMR spectra may be obtained in the solid state[4] by the combined use of "dilute" nuclei to minimize homonuclear interactions, dipolar decoupling to remove dipolar interactions to protons, and magic angle spinning[5] to average the shift anisotropies to their isotropic values. In addition, cross-polarization techniques[6] may be used to increase S/N.[7] In the case of many inorganic systems (including zeolites), there are no protons covalently bonded to the aluminosilicate framework, and the experiment reduces to the very simple one of MAS alone, which can be performed at high magnetic field strengths using conventional high-resolution equipment.[8]

In recent years, $^{29}Si/^{27}Al$ MAS NMR spectroscopy has emerged as a complementary technique to X-ray diffraction measurements for the investigation of zeolite crystal structures.[9] In the case of low Si/Al ratio materials, five resonances are observed (to a first approximation), corresponding to the five possible local environments Si[4Al], Si[3Al, Si], Si[2Al, 2Si], Si[Al, 3Si], and Si[4Si] describing the (average) Si/Al distribution throughout the framework. In completely siliceous materials where only the Si[4Si] local environment is present, very sharp resonances are observed, which are due to the crystallographically inequivalent silicon sites in the unit cell and whose relative intensities reflect the relative site occupancies.[10] These latter spectra may thus be directly related to the results of diffraction experiments.

In solution NMR studies, the application of 2D techniques has provided a wealth of information on the two-dimensional connectivities between atoms within molecular structures.[11] For example, the HSC (heteronuclear shift correlation) sequence establishes heteronuclear connections such as $^{13}C/^{1}H$, $^{29}Si/^{1}H$, etc., the COSY sequence defines homonuclear correlations, such as $^{1}H/^{1}H$, $^{31}P/^{31}P$, $^{29}Si/^{29}Si$, etc., the INADEQUATE sequence $^{13}C/^{13}C$ in natural abundance, while longer range connectivities, such as $^{1}H/^{1}H/^{13}C$, can be probed by the RCT (relayed coherence transfer) sequence.

A number of 2D NMR experiments have been introduced in high-resolution solid-state NMR studies, for example, to investigate chemical exchange processes,[12] retrieve chemical shift anisotropies[13] and dipolar couplings,[14] and probe spin-diffusion processes.[15] Opella has proposed an internuclear distance-determined spin-diffusion mechanism in molecular crystals,[16] and

* Authors to whom correspondence should be addressed.
† On leave from Mineralogisches Institut der CAU, 23 Kiel, FRG.

(1) (a) Breck, D. W. *Zeolite Molecular Sieves*, Wiley-Interscience: New York, 1974. (b) Smith, J. V. *Zeolite Chemistry and Catalysis*; Rabo, J. A., Ed.; ACS Monograph 171, American Chemical Society: Washington 1976; p 3.

(2) (a) Barrer, R. M. *Zeolites and Clay Minerals as Sorbents and Molecular Sieves*; Academic Press: London, 1978. (b) Holderich, W.; Hesse, M.; Näumann, F. *Angew. Chem.* **1988**, *27*, 226.

(3) (a) Information from powder diffraction data may be improved by use of Rietveld analysis and synchrotron X-ray sources. (b) The use of synchrotron X-ray sources also makes it possible to work with much smaller crystals and may be generally applicable to zeolites in the future: Eisenberger, P.; Newman, J. B.; Leonowicz, M. E.; Vaughan, D. E. W. *Nature* **1984**, *309*, 45.

(4) A description of the range of applications of these experiments in chemical systems is given in: Fyfe, C. A. *Solid State NMR for Chemists*; CFC Press: 1984.

(5) (a) Andrew, E. R.; Bradbury, A.; Eades, R. G. *Nature* **1958**, *182*, 1659. (b) Lowe, I. J. *Phys. Rev. Lett.* **1959**, *2*, 285.

(6) Pines, A.; Gibby, M. G.; Waugh, J. S. *Chem. Phys. Lett.* **1972**, *15*, 273.

(7) Schaefer, J.; Stejskal, E. O. *J. Am. Chem. Soc.* **1978**, *98*, 1031.

(8) Fyfe, C. A.; Gobbi, G. C.; Hartmann, J. S.; Lenkinski, R. E.; O'Brien, J. H.; Beange, E. R.; Smith, M. A. R. *J. Magn. Reson.* **1982**, *47*, 168.

(9) Engelhardt, G.; Michel, D. *High Resolution Solid-State NMR of Silicates and Zeolites*; Wiley: New York, 1987.

(10) Fyfe, C. A.; Gobbi, G. C.; Murphy, W. J.; Ozubko, R. S.; Slack, D. A. *J. Am. Chem. Soc.* **1984**, *106*, 4435.

(11) (a) Benn, R.; Günther, H. Modern Pulse Methods in High Resolution NMR Spectroscopy. *Angew. Chem., Int. Ed. Engl.* **1983**, *22*, 250. (b) Bax, A. *Two Dimensional Nuclear Magnetic Resonance in Liquids*; Delft University Press: Delft, The Netherlands, 1982. (c) Derome, A. E. *Modern NMR Techniques for Chemistry Research*; Pergamon Press: Oxford, England, 1987. (d) Sanders, J.; Hunter, B. *Modern NMR Spectroscopy, A Guide for Chemists*; Oxford University Press: Oxford, England, 1987.

(12) Szeverenyi, N. M.; Sullivan, M. J.; Maciel, G. E. *J. Magn. Reson.* **1982**, *47*, 462.

(13) Bax, A.; Szeverenyi, N. M.; Maciel, G. E. *J. Magn. Reson.* **1983**, *51*, 400.

(14) (a) Opella, S. J.; Waugh, J. S. *J. Chem. Phys.* **1977**, *66*, 4919. (b) Bodenhausen, G.; Stark, R. E.; Ruben, D. J.; Griffin, R. G. *Chem. Phys. Lett.* **1979**, *67*, 424.

(15) Caravatti, P.; Deli, J. A.; Bodenhausen, G.; Ernst, R. R. *J. Am. Chem. Soc.* **1982**, *104*, 5506.

(16) Frey, M. H.; Opella, S. J. *J. Am. Chem. Soc.* **1984**, *106*, 4942.

0002-7863/89/1511-7702$01.50/0

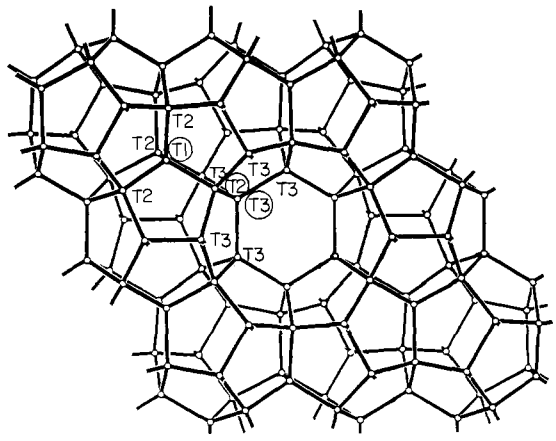

Figure 1. Schematic representation of the zeolite ZSM-39 lattice framework. The three crystallographically inequivalent tetrahedral lattice sites are indicated by T_1, T_2, and T_3 (inside circles), and in each case the identities of the four nearest neighbors are shown.

Benn and co-workers have recently demonstrated C/H connectivities using the INADEQUATE sequence for the plastic crystal camphor and have used the COSY sequence for $^{29}Si/^{29}Si$ connectivities in the reference molecule Q_8M_8.[17]

At least in principle, 2D NMR techniques can be used to establish connectivities in the solid state, and for crystalline three-dimensional framework (lattice) structures (in contrast to the case of molecular crystals), these connectivities could be used to define the three-dimensional lattice itself. In the present work, we examine the potential of 2D ^{29}Si NMR measurements involving spin-diffusion and scalar coupling interactions to establish three-dimensional Si/O/Si lattice connectivities in zeolite framework structures. A preliminary account of this work has been presented.[18]

Experimental Section

^{29}Si MAS NMR spectra were obtained at 79.49 MHz using a Bruker MSL 400 spectrometer. 2D spin-diffusion experiments were performed as described by Maciel and co-workers[12] using a standard ^1H to ^{29}Si cross-polarization to initiate the sequence. Spin diffusion from individual resonances was investigated as described by VanderHart[19a] using a DANTE sequence to invert the selected resonance during the "mixing" period.[19b] 2D COSY experiments were carried out using a conventional sequence,[20] except that it was again initiated by a ^1H to ^{29}Si cross-polarization step. Further details of the pulse sequences and the acquisition parameters used are given in the text.

A completely siliceous sample of dodecasil-3C (ZSM-39) was synthesized hydrothermally in a sealed silica glass tube in 8 days at 200 °C using piperidine as template, with a quantitative yield. The silica source was enriched to approximately 80% in ^{29}Si to increase the number of $^{29}Si/O/^{29}Si$ interactions as much as possible.

Results and Discussion

Sample Description. In order to investigate the potential of high-resolution solid-state NMR techniques, a system of known structure was chosen and synthesized in such a form as to facilitate the application of both spin-diffusion and scalar coupling experiments.

Zeolite ZSM-39 (clathrasil dodecasil-3C) is a highly siliceous porous tectosilicate (network system) whose crystal structure was proposed by Kokotailo and co-workers[21] and refined in detail by Gies[22] (Figure 1). The space group symmetry of the high-temperature form of the compound is *Fd*3. There are 136 atoms tetrahedrally coordinated by oxygen (T atoms) in the unit cell distributed over three sites T_1, T_2, and T_3 (8:32:96), of relative proportions (1:4:12). (Throughout the manuscript bold letters will be used to denote the T sites T_1, T_2, and T_3 to avoid confusion with T_2 and T_1, the spin–spin and spin–lattice nuclear spin relaxation times. Both designations are accepted usage in their respective areas.) The room-temperature form of the as-synthesized material is tetragonal and deviates from cubic symmetry by the absence of the 3-fold symmetry axis. Therefore, the degeneracy of the T_3 site is lifted, and there are three very similar sites T_3', T_3'', and T_3''' of relative proportions 32:32:32. Figure 1 shows the location of the different T sites in the lattice and their relationship to each other. The connectivities between the T sites are the following: T_1 is connected to 4 T_2 sites; T_2 is connected to 1 T_1 and 3 T_3 sites; T_3 is connected to 1 T_2 and 3 T_3 sites. Within the unit cell there are, therefore, omitting self-connectivities, 32 T_1T_2 connectivites, 96 T_2T_3 connectivities, and no direct connectivities between T_1 and T_3.

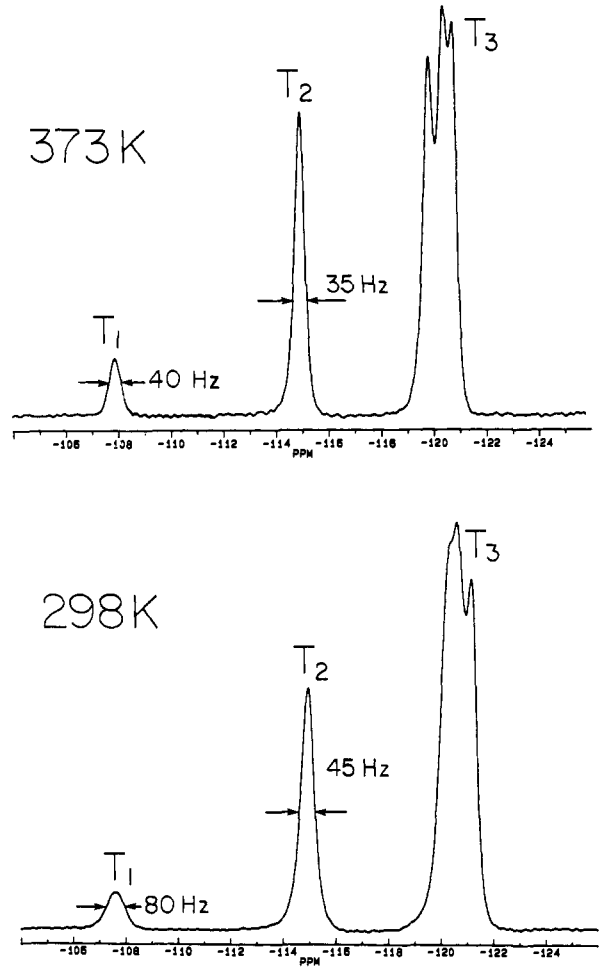

Figure 2. ^{29}Si CP/MAS NMR spectra of the sample of ^{29}Si-enriched ZSM-39 used in these studies at the temperatures indicated.

The ^{29}Si CP MAS spectrum of the ^{29}Si-enriched sample prepared for these studies is shown in Figure 2. The three T sites are clearly resolved, and the structure of the T_3 resonance reflects the absence of a 3-fold symmetry axis. The resonances are quite narrow (e.g., ~40 Hz, ~0.5 ppm for the T_2 site), indicating that the system is both highly siliceous and highly crystalline and also fault-free. This is important for scalar coupling experiments, especially those involving small couplings as the maximum time allowed in the simple experiment for frequency encoding and the establishment of scalar coupling effects will be determined by the T_2^* relaxation times of the nuclei being observed. The T_2^* values of the ^{29}Si resonances of this sample are 10 ms or less. In order to carry out spin-diffusion measurements, it is desirable to have long T_1 values for the nuclei being observed. The ^{29}Si T_1 relaxation

(17) Benn, R.; Grondey, H.; Brevard, C.; Pagelot, A. *J. Chem. Soc., Chem. Commun.* **1988**, 102.
(18) Fyfe, C. A.; Gies, H.; Feng, Y. *J. Chem. Soc., Chem. Commun.*, in press.
(19) (a) VanderHart, D. L. *J. Magn. Reson.* **1987**, *72*, 13. (b) Caravatti, P.; Bodenhausen, G.; Ernst, R. R. *J. Magn. Reson.* **1983**, *55*, 88.
(20) Muller, L.; Kumar, A.; Ernst, R. R. *J. Chem. Phys.* **1975**, *63*, 5490.
(21) Schlenker, J. L.; Dwyer, F. G.; Jenkins, E. E.; Rohrbaugh, W. J.; Kokotailo, G. T.; Meier, W. M. *Nature* **1981**, *294*, 340.
(22) Gies, H.; Liebau, F.; Gerke, H. *Angew. Chem.* **1982**, *94*, 214.

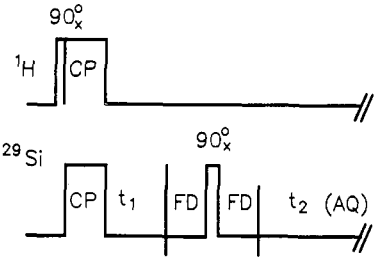

Figure 3. Schematic representation of the modified COSY experiment used in the present work.

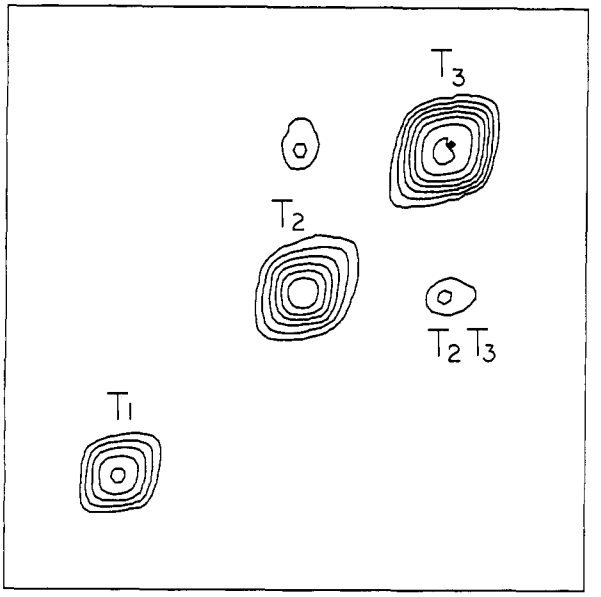

Figure 4. Contour plot of COSY experiment carried out at ambient temperature using the pulse sequence of Figure 3 with 128 experiments, 48 scans in each experiment, sweep width of 5 kHz, and 256 data points collected during the acquisition. The fixed delay was 15 ms and the total experimental time approximately 17 h. Sine bell squared apodization was used and the plot symmetrized.

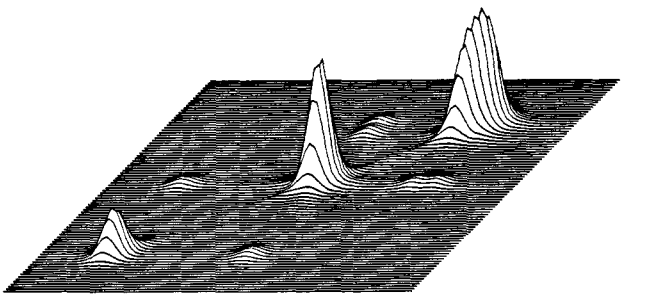

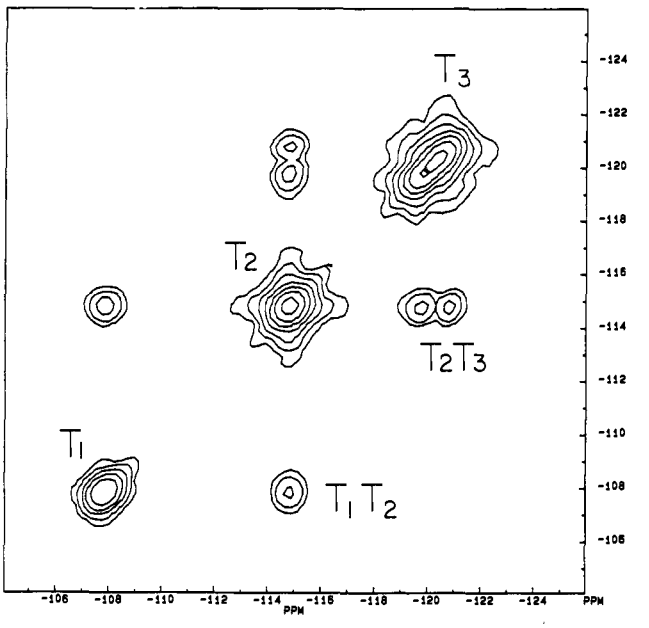

Figure 5. Contour and stacked plots of a 2D COSY experiment on ZSM-39 at 373 K using the pulse sequence of Figure 3 with 128 experiments, 64 scans in each experiment, 5-kHz sweep width, 256 data points on acquisition, and a fixed delay of 5 ms. Sine bell apodization was used, and the data are presented without symmetrization or smoothing. The total experimental time was approximately 23 h.

time values of the present sample are approximately 650 s and impose no constraints on the delay used. However, because of this, it is important to be able to use cross-polarization techniques, which depend only on the ^1H spin–lattice relaxation time T_{1H}, so as to minimize the delay time between acquisitions. As can be seen from Figure 2, they work very well in the present instance, the proton T_1 value of the template of approximately 3 s giving a very time-efficient experiment.

COSY Experiments. Although connectivities based on scalar couplings are the most unambiguous because the couplings are through connecting bonds, there are a number of related difficulties in performing these experiments in the solid state, which for silicates are quite severe. Thus, in the pulse sequence that was used shown in Figure 3, the frequency encoding is established in the period t_1 whose maximum duration will be limited effectively by the spin–spin relaxation time T_2 of the ^{29}Si nuclei. In solution this will not be a severe limitation because of the relatively similar values of T_1 and T_2, but in the solid state, these two relaxation times will usually be quite different. Even in spectra where the resonances are narrow enough to resolve chemically inequivalent nuclei (so-called "good resolution"), the T_2^* values of the resonances will often be quite short, of the order of tens of milliseconds or less. For directly bonded nuclei where the couplings are large, this will not be too limiting, but in the case of silicates, the connectivities are through two bonds (^{29}Si–O–^{29}Si) and are known from solution NMR studies to be of the order of 1–10 Hz in most cases.[23] For small couplings like these, even longer evolution times are preferable, but these will not be possible for short T_2^* values. In addition, since the couplings are not directly observable, it is not possible to carry out the corresponding 1D experiments. It should be noted that the ^{29}Si resonances of Q_8M_8, the one molecular crystal in which $^{29}Si/O/^{29}Si$ connectivities have been demonstrated, are atypically narrow, allowing long evolution times.[17] A preliminary series of 2D COSY experiments was carried out with 128 frequency encoding increments to ensure adequate resolution with total encoding time periods of up to ~50 ms. Figure 4 shows the best results obtained with the parameters given in the figure caption in this first series of experiments. As seen in the figure, a clear connectivity is established between T_2 and T_3 but the expected interaction between T_1 and T_2 is not observed. Although the intensity of the T_1 resonance is considerably less than the others and the number of interactions is 3 times lower than for T_2T_3, the S/N of the 2D plot is such that the T_1T_2 cross-peak should have been observable if it had had a similar growth profile. (It is also possible that the scalar couplings between T_1 and T_2 are less than those between T_2 and T_3, reducing the efficiency of the interaction to the point where the cross-peak is not observable.) Just as in solution studies, the observation of a cross-peak indicates a connectivity, but the nonappearance of a cross-peak is uninformative.

However, it is also possible that the T_2^* relaxation time of the T_1 resonance is shorter than those of the other resonances. Inspection of Figure 2 reveals that the width of the T_1 resonance is approximately twice that of the other signals (~80 vs ~40 Hz),

(23) Harris, R. K.; O'Connor, M. J.; Curzon, E. H.; Howarth, O. W. *J. Magn. Reson.* **1984**, *57*, 115.

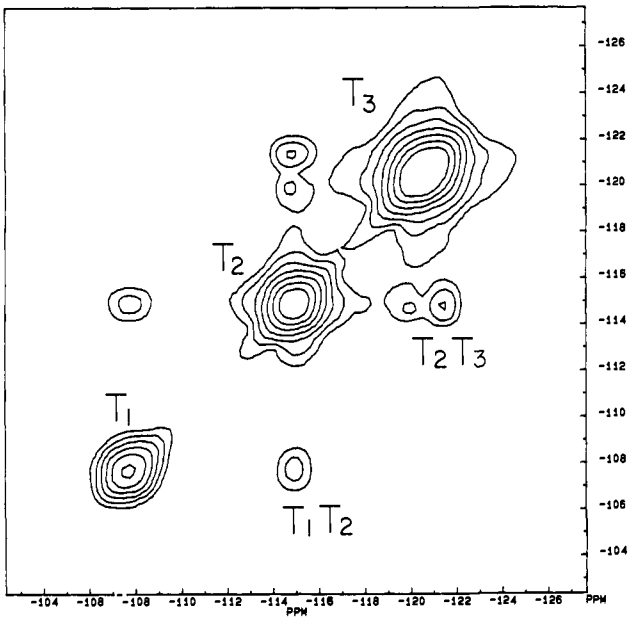

Figure 6. Contour plot of 2D COSY experiment on ZSM-39 at 298 K: 64 experiments, 80 scans/experiment, 5-kHz sweep width, fixed delay of 2 ms, and 256 data points collected during the acquisition. Sine bell apodization was used, and the plot has been symmetrized and a smoothing function applied. Total experiment time was approximately 14 h.

suggesting a shorter T_2* value for this nucleus, which could adversely affect the experiment. In an attempt to narrow the resonances, the sample temperature was raised while monitoring the spectra. By 373 K the line width of the T_1 resonance was reduced to ~40 Hz while those of the other resonances were ~35 Hz, Figure 2. The results of a ^{29}Si COSY experiment at 373 K obtained using the same experimental parameters as used previously are shown in Figure 5. In addition to the T_2T_3 cross-peaks previously observed, T_1T_2 cross-peaks are now clearly visible, although of somewhat lower intensity. The doubling of the T_2T_3 cross-peak is real and is due to the partial resolution of the T_3 resonance due to the absence of cubic symmetry. There is almost no difference in the 2D plot whether symmetrization is used or not, attesting to the reliability of the experiment. These results are in exact agreement with the known connectivities of the structure and confirm not only the structure itself but also the importance of the T_2* relaxation times in this solid-state experiment in its simplest form as in Figure 3.

Variation of the fixed delay time showed that the best results were obtained with a total fixed delay of 10 ms and total maximum encoding time of 36 ms for 128 frequency encoding experiments (t_1 variation) but that clear T_1T_2 and T_2T_3 correlations were obtained over the range of 30–56 ms for the maximum t_1 encoding time.

When we used this information and estimated that T_2* of the T_1 resonance at room temperature was reduced to approximately half of its high-temperature value, a COSY experiment was again attempted at ambient temperature but with the number of experiments reduced to 64 to half the encoding time. Both T_1T_2 and T_2T_3 correlations are clearly observed over a range of maximum encoding times (including fixed delays) of 13–23 ms, with the best data obtained at a value of 17 ms (total fixed delay 4 ms; Figure 6). In these cases, although the connectivities are clearly observable without symmetrization, this procedure considerably improves the quality of the plots. The degradation in the quality of the correlations at ambient temperatures may be recovered by, in part, the use of COSY 45 or double-quantum filtered (DQF) COSY experiments. This is illustrated in Figure 7, which shows the results of a DQF COSY experiment with 64 frequency encoding increments where the quality of the connectivities is almost completely recovered. It is even possible to observe both connectivities when the number of frequency encoding experiments is reduced to 32, but considerable care must be taken in the application of the symmetrization procedure to ensure that it does not introduce specious correlations arising from t_1 and other noise. It does suggest, however, that ^{29}Si/O/^{29}Si connectivity

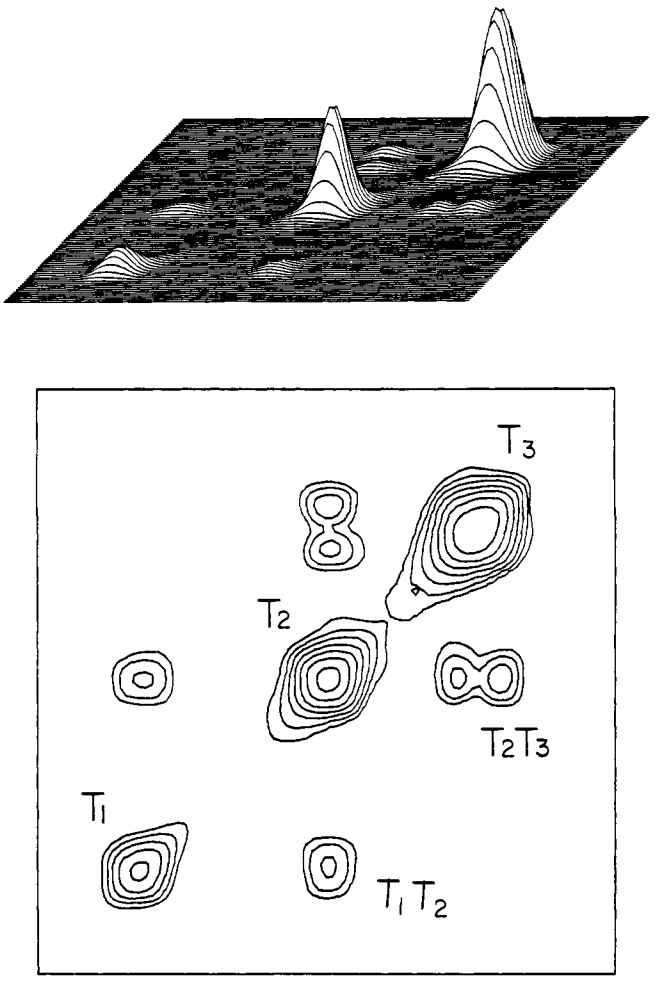

Figure 7. Contour and stacked plots of a DQF COSY experiment on ZSM-39 at 298 K: 64 experiments, 128 scans/experiment, 5-kHz sweep width, 256 data points on acquisition, and a fixed delay of 2 ms. Sine bell squared apodization was used, and the plots have been symmetrized and smoothed. Total experimental time was approximately 23 h.

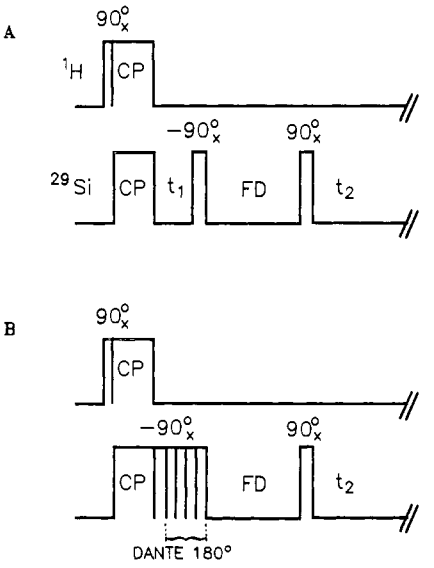

Figure 8. Schematic representation of the pulse sequences used for spin-diffusion measurements: (A) one-dimensional sequence with selective inversion of one resonance using a DANTE sequence; (B) two-dimensional spin-diffusion sequence.

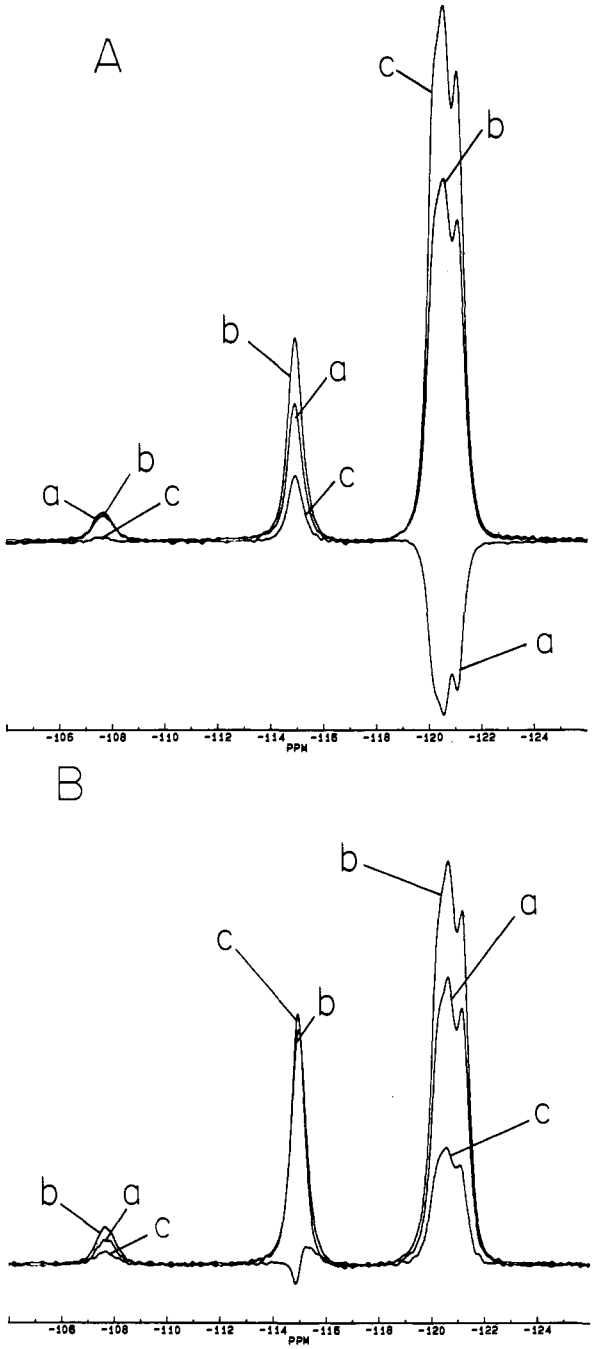

Figure 9. One-dimensional experiments using the pulse sequence of Figure 7A illustrating spin diffusion from individual resonances as indicated; 8 scans were taken in each experiment with a contact time of 20 ms (see text for further details): (A) inversion of T_3 resonance, fixed delay 1 s. (B) inversion of T_2 resonance, fixed delay 5 s.

information may be obtained from experiments of this type in a variety of systems with line widths up to ~200 Hz (~2 ppm at 9.4 T), especially if modified COSY experiments are used.

Even better information could have been obtained if the ^{29}Si T_2^* relaxation time values had been longer, and it may well be that correlations based on scalar couplings will be most successful when carried out on samples with the narrowest possible resonances (line widths as low as 6 Hz have been reported),[24] even if this means working with natural abundance samples with the attendant severe loss in sensitivity.

Spin-Diffusion Experiments. The attraction of spin-diffusion measurements as probes of lattice connectivities comes from the steep internuclear distance dependence of the interaction (other

(24) Strobl, H.; Fyfe, C. A.; Kokotailo, G. T.; Pasztor, C. T. *J. Am. Chem. Soc.* **1987**, *109*, 7433.

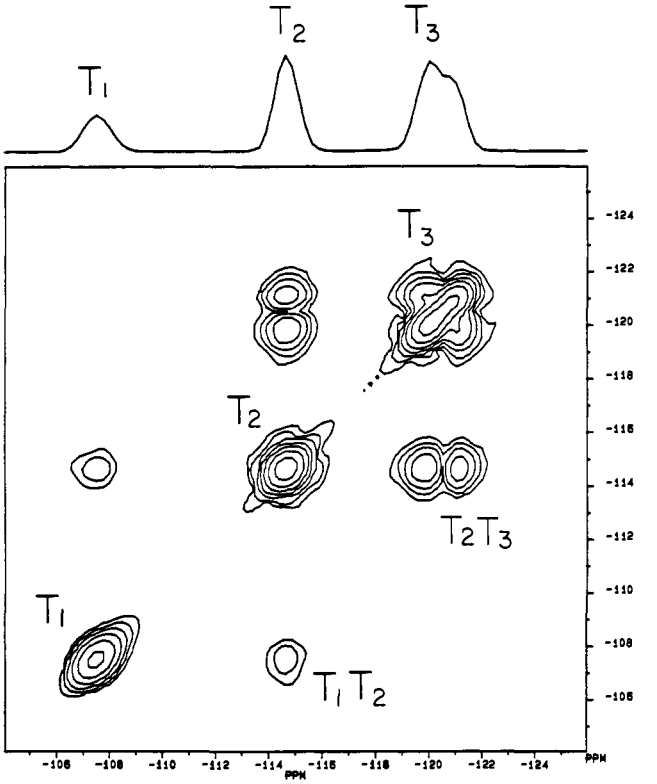

Figure 10. Contour plot of 2D spin-diffusion experiment using the pulse sequence of Figure 7B with 128 experiments, 8 scans in each experiment, sweep width of 5 kHz, and 256 data points collected during acquisition. The fixed delay during which spin diffusion occurs was 10 s, the spinning rate 2 kHz, and the total time for the experiment approximately 6 h. Sine bell squared apodization was used, and the plot has been symmetrized.

contributions and possible complications will be discussed subsequently). Since ^{29}Si–O^{29}Si distances are all approximately 3.1 Å while ^{29}Si–O–Si–O^{29}Si distances are approximately 5.4 Å in these systems, it was hoped that the two would be clearly differentiated. As can be seen from a consideration of the pulse sequences of Figure 8 that the determining relaxation time in the delay period is T_1 of the ^{29}Si nuclei. In the present instance, this is of the order of 650 s and imposes no limitations on the experiment, while the ability to generate the ^{29}Si magnetization via a cross-polarization sequence means that the experiment will be an efficient one, the repeat time between pulse sequences depending only on the proton T_1, which is of the order of 3 s.

Figure 9 shows the magnetization transfers from each of the two larger resonances at mixing times of 1 and 5 s as indicated by using the pulse sequence of Figure 8A.[19] In this experiment, when the magnetization is stored along z after the frequency encoding step, the magnetization of one of the resonances is selectively inverted to $-z$. After a time, application of a 90°x pulse reestablishes the magnetization in the xy plane where the FID is recorded. In Figure 9, curve a represents the spectrum after a fixed delay but with the transmitters gated off during the DANTE period, curve b after the same fixed delay but with a 180° DANTE pulse, and curve c the difference, which reflects the progress of the spin-diffusion process. As can be seen from the figures, there is relatively rapid spin-diffusion between T_2 and T_3 and between T_2 and T_1 while that between T_1 and T_3 is much slower, in agreement with the known connectivities in the structure. The spin-diffusion experiment can also be performed in a two-dimensional manner[12] using the pulse sequence of Figure 8B as shown in Figure 10 for a mixing time of 10 s. In agreement with theoretical predictions, the efficiency of the spin-diffusion process increases as the spinning rate is lowered. At long spin-diffusion periods (25 s at 2-kHz spinning frequency) or shorter times at lower spinning rates (5–10 s at 1 kHz), spin diffusion is eventually observed between T_1 and T_3, as would be expected. However,

although the results of the spin-diffusion experiments shown in Figures 9 and 10 fit exactly with the (known) connectivities in the structure, some caution must be exercised in their interpretation in terms of three-dimensional connectivities in the structure. The theory of spin diffusion between dilute nuclei has been described by Ernst[25] and by McDowell,[26] Clayden,[27] and Henrichs et al.[28] and discussed in terms of its use in probing internuclear distances by VanderHart.[19a] In the recent paper by McDowell and Kubo, the interactions involved in spin diffusion under MAS conditions are discussed in detail.[26b] The rate of spin diffusion is strongly dependent on internuclear distance ($\alpha l/r^6$), but it is also dependent on the frequency separations of the isotropic chemical shifts and the magnitudes and relative orientations of the shift anisotropy patterns of the nuclei involved. Since the latter element will in general be undefined, its contribution to the spin-diffusion process will be unknown. Because all of the silicon nuclei are in tetrahedral environments and have relatively small shift anisotropies, it is probably unlikely that this effect will dominate the spin-diffusion process, but studies of a number of additional systems will be necessary to confirm this at least on an empirical basis.

Conclusions

For the sample of ZSM-39 investigated, 2D NMR experiments based both on scalar couplings and on spin diffusion yield information on $^{29}Si/O/^{29}Si$ connectivities in exact agreement with the known crystal structure and suggest that these techniques may be of general use in the determination of zeolite crystal structures. Further, experiments based on scalar couplings will be best carried out on samples that exhibit the narrowest resonances possible (and correspondingly long T_2 and T_2^* values) in order to permit the longest possible evolution times for the small scalar couplings involved, although positive results could be obtained for resonances of up to 2 ppm. Spin-diffusion experiments yielded the correct connectivities for the lattice structure investigated, but work on other systems will be needed in order to establish more clearly the reliability of these experiments in this context due to unknown contributions of non-distance-dependent factors. Further work based on these conclusions is currently in progress. Although, in general, ^{29}Si enrichment facilitates the experiments, the expense involved obviously limits their general application. By paying careful attention to the importance of the T_2 or T_2^* values in these experiments, we have been able in preliminary work to apply these techniques to natural-abundance samples in the form of COSY and INADEQUATE experiments and to observe the $^{29}Si/^{29}Si$ couplings directly.[29] Although the experiments are very demanding and time consuming, in terms of both sample preparation and the spectroscopy involved, the wealth of information potentially available makes them attractive additions to the techniques currently available for investigating three-dimensional lattice structures.

Acknowledgment. We acknowledge the financial assistance of the NSERC (Canada) in the form of operating and equipment grants (C.A.F.) and the Alexander Von Humboldt Foundation (H.G.). C.A.F. acknowledges the award of a Killam Research Fellowship from the Canada Council and Y.F. a University Graduate Fellowship.

(25) Suter, D.; Ernst, R. R. *Phys. Rev. B* **1982**, *25*, 6038; **1985**, *32*, 5608.
(26) (a) Kubo, A.; McDowell, C. A. *J. Chem. Phys.* **1988**, *89*, 63. (b) Kubo, A.; McDowell, C. A. *J. Chem. Soc., Faraday Trans. 1*, in press.
(27) Clayden, N. J. *J. Magn. Reson.* **1986**, *68*, 360.
(28) Henrichs, P. M.; Linder, M.; Hewitt, J. M. *J. Chem. Phys.* **1986**, *85*, 7077.
(29) Fyfe, C. A. and co-workers. Work in progress.

^{15}N NMR Study on Cyanide ($C^{15}N^-$) Complex of Cytochrome P-450$_{cam}$. Effects of *d*-Camphor and Putidaredoxin on the Iron–Ligand Structure

Yoshitsugu Shiro,*,† Tetsutaro Iizuka,† Ryu Makino,‡ Yuzuru Ishimura,‡ and Isao Morishima§

Contribution from the Institute of Physical and Chemical Research, Wako-shi, Saitama 351-01, Japan, Department of Biochemistry, School of Medicine, Keio University, Shinanomachi, Shinjuku, Tokyo 160, Japan, and Division of Molecular Engineering, Graduate School of Engineering, Kyoto University, Kyoto 606, Japan. *Received February 15, 1989*

Abstract: The cyanide ($C^{15}N^-$) complex of *Pseudomonas putida* cytochrome P-450 (P-450$_{cam}$) exhibited well-resolved and hyperfine-shifted ^{15}N NMR resonances arising from the iron-bound $C^{15}N^-$ at 423 and 500 ppm in the absence and presence of the substrate, *d*-camphor, respectively. The values were smaller than those for cyanide complexes of myoglobin and hemoglobin (~1000 ppm) but fell into the same range as those for the cyanide complexes of peroxidases (~500 ppm). The ^{15}N shift values of P-450$_{cam}$ were not incompatible with the existence of anionic ligand, such as cysteinyl thiolate anion, at the fifth coordination site of heme iron. The difference in the ^{15}N chemical shift values between camphor-free and -bound enzymes was inferred by the increase in the steric constraint to the Fe–C–N bond upon substrate binding. When putidaredoxin was added to the $C^{15}N^-$ complex of camphor-bound P-450$_{cam}$, the ^{15}N NMR signal changed from 500 to 477 ppm. The spectral changes were interpreted in terms of the structural changes in the vicinity of iron-bound ligand and discussed in relation to the functional properties of P-450$_{cam}$.

Cytochrome P-450 is a generic name given for b-type cytochrome, which exhibits Soret absorption at 450 nm upon complex formation with CO. The enzyme P-450 acts as a terminal oxidase in the monooxygenation reaction and cleaves dioxygen into a water and a single oxygen atom, which is inserted into a hydrocarbon bond. Recent X-ray crystallographic studies[1] of *Pseudomonas putida* cytochrome P-450 (P-450$_{cam}$) clearly showed that the substrate molecule, *d*-camphor, is buried in an internal pocket just

* To whom correspondence should be addressed.
† The Institute of Physical and Chemical Research.
‡ Keio University.
§ Kyoto University.

(1) (a) Poulos, T. L.; Finzel, B. C.; Gunsalus, I. C.; Wagner, G. C.; Kraut, J. *J. Biol. Chem.* **1985**, *260*, 16122–16130. (b) Poulos, T. L.; Finzel, B. C.; Howard, A. J. *J. Mol. Biol.* **1987**, *195*, 687–700.

0002-7863/89/1511-7707$01.50/0